VLASS Memo no. 23
Direction-dependent calibration for VLASS observation

Viral Parekh
vparekh@nrao.edu
National Radio Astronomy Observatory, Socorro, NM

May 30, 2024

Abstract: In this memo, we have applied the direction-dependent (DD) calibration technique to the VLA Sky Survey (VLASS) data using CASA and QuartiCAL software. In the VLASS quick-look (QL) image archive, 10% or more quality assurance (QA) process rejected maps have strong and compact radio sources that cause artifacts and hamper the detection of faint radio sources. We developed a Python script using CASA and QuartiCAL software and performed "peeling" to some of the VLASS data. Quartical is third-party software and is not maintained by the NRAO (and CASA team), but one can install it in the CASA virtual environment and use it along with CASA's tasks to do the calibration. Quartical can be used to do both direction-independent (DI) and direction-dependent calibration. After peeling, we found significant improvements in VLASS images. This peeling with QuartiCAL is an automated technique and one can select multiple strong sources for DD calibration. QuartiCAL can solve DD gains for all of these sources simultaneously and generate residual columns after subtracting problematic sources, for further imaging. This method can be integrated into the VLA pipeline or used independently inside the CASA environment. Previously, we used the peeling technique (but not in CASA or with `tclean`) for VLA, MeerKAT, and uGMRT single-pointing observations, which only have single-field data with long exposure. Here, for the first time, we are performing DD calibration for mosaic OTF VLA data and found that this technique can improve image quality (more than a factor of 5 improvement in rms around bright source) and dynamic range of VLASS data.

1 Background

VLA Sky Survey (VLASS) is the S-band (2–4 GHz) all-sky survey (dec $> -40°$) conducted in three epochs (Lacy et al., 2020). The first epoch (VLASS 1) was completed in 2019, the second (VLASS 2) was completed in 2022 and the third (VLASS 3) was completed in 2024. Over these years NRAO (VLASS-team) has provided quick-look (QL) images to the community. Some of these QL maps are not used to derive scientific results because of their poor quality. The VLASS team has recently provided single-epoch (VLASS 2.1 and 2.2) self-calibrated (SE) images. However, some of the quality assurance (QA) rejected maps are not processing for self-calibration because of the poor rms and bright source(s) in the field causing strong artifacts in maps, and preventing to achieve high-dynamic range (HDR) imaging. We took some of these maps and applied direction-dependent (DD) calibration to reduce the artifacts and improve DR[1]. The aim of the work is to (1) test and develop the DD calibration technique for VLASS (and on-the-fly (OTF)/mosaic mode data), (2) develop the flexible and user-friendly DD calibration method with CASA and

[1]We used the standard definition of DR is peak/rms.

incorporate it in VLA pipelines and (3) improve the image quality of the VLA data and support the users to make quality maps to achieve their scientific goals.

High-sensitive radio interferometric observations, for example with VLA, MeerKAT, LOFAR, etc. are wide-field and wide-bandwidth capable of detecting many bright and faint sources simultaneously. If any bright source(s) ($>$ 100 mJy), in the observation, is not characterized by the calibration process, and due to the imperfect primary beam of the telescope, it limits the dynamic range by throwing strong artifacts during imaging. Further, the central portion of the primary beam is corrupted by this bright source located at the edges; which corrupts PSF and/or dominates selfcal gain solutions. This will hamper the detection of faint emissions in the presence of strong artifacts due to calibration errors. VLASS uses the OTF imaging mode, so the telescope is continuously moving while sampling the sky brightness distribution. The bright and poorly deconvolved source is also moving in the primary beam for each of the fields in the data. This makes calibration more challenging. "Peeling" is one of the DD calibration techniques widely used in MeerKAT and LOFAR data reduction pipelines to improve image quality.

1.1 DD calibration with QuartiCAL

QuartiCAL (Kenyon et al., 2025)[2] is a successor to the CubiCal package (Kenyon et al., 2018), which employs complex optimization routines to perform fast radio interferometric calibration. But, QuartiCAL improves upon CubiCAL, in terms of both flexibility and performance. QuartiCAL is a novel Python package and it can carry out both DI and DD calibrations by applying simultaneous multiple gain terms (complex, delay, phase, leakage, feed rotation, etc.) to the data. Similar to the CubiCal, QuartiCAL also performs DD calibration using a simultaneous form of the 'peeling' approach called *differential-gains* (Smirnov, 2011a). It can apply corrections to many sources simultaneously from the self-calibrated sky model, unlike the one-by-one iterative algorithm used by the typical peeling method (Williams et al., 2019). These sources are manually marked and contain information on the specific direction in which to perform peeling. In QuartiCAL, the Radio Interferometer Measurement Equation (RIME, Smirnov (2011a,b)) used for the differential gains takes the form:

$$D_{l,m} = G_l \Bigg(\sum_{l,m} \sum_{s} \Delta E_l P_l K_l S_{l,m,s} K_m^H P_m^H \Delta E_m^H \Bigg) G_m^H \tag{1}$$

G are direction-independent errors affecting the entire FOV, constrained to phase-only solutions while ΔE are direction-dependent errors that are notably present around strong sources far away from the phase center. These errors are constrained to fully complex 2×2 Jones matrices. P terms are implemented for antenna-specific primary beam models to correct for time and frequency-varying gains, K terms represent delay (frequency slope as a function of time and spectral windows) and S terms denote sky models or clean component models of the given observation. K term is implemented to solve for errors related to visibility phases, generated by the atmosphere, signal paths, or other pre-calibration steps. The sum is over all sources S and their respective directions l, m. QuartiCAL solves for the G terms (DI) on small-time/frequency scales by the field as a whole while simultaneously solving for ΔE terms (DDE) on larger time/frequency scales for a subset of sources. The advantage of using the above RIME is that most of the clean components or all-sky flux are taken into account while solving direction-dependent gains. This, to a large extent, avoids the flux suppression typically observed in the self-calibration (a&p) process. This RIME equation also ensured that direction-independent gains were not affected by flux variability because of the effects of the antenna's far-field response on bright off-axis sources.

[2] `https://quartical.readthedocs.io/en/latest/`

2 "Peeling" method in CASA

Various pipelines and data analysis suites use different methods for peeling the bright source(s) from radio interferometric observations. We have also shown this method for VLA data in VLA Memo 231. In the previous work, we used DDFacet, WSClean, and CubiCal software. These special packages, mainly imagers, are external (not in CASA) and cannot be used with VLA pipelines in a single run. Also, the user has to install them into their system or needs to use docker-based images. It is also difficult to use these external tools in the CASA environment. We developed a method to do peeling with QuartiCAL software inside the CASA environment along with internal tasks such `tclean` imager. QuartiCAL is a flexible and powerful calibration tool that can be implemented in VLA pipelines. Here we show how to do peeling inside the CASA.

1. As described in VLA memo 231, one needs to first generate the all-sky model using regular self-calibration. In the last run of self-cal, it will generate a self-calibrated 'CORRECTED_DATA' column and corresponding sky model in the 'MODEL_DATA' column in the measurement set (MS).

2. We can start DD calibration with these two columns. One can also start with final self-calibrated visibility (typically output from imaging pipeline) and run again `tclean` task on it with their choice of imaging parameters (e.g. robust weighting, uvrange, Taylor terms, user supply mask, etc.) and predict the new model into the MODEL_DATA column.

3. 'QuartiCAL' takes multiple model data columns - one is for all sky models (direction-independent or direction zero) and the second is for problematic bright sources (direction-dependent or direction one). Since CASA only accepts one MODEL_DATA column in the MS, we need to copy the MODEL_DATA column for each of the directions into the user-defined column names. For example, after running `tclean` on self-calibrated MS, we copy the MODEL_DATA into the ALL_SKY_MODEL column.

4. Every time we need to generate and add the new column into MS to copy the MODEL_DATA in it. If there is more than one bright source that needs to be peeled, then the user has to generate those many model data columns (each for the source) in the MS, for example, Bright_Source_col1, Bright_Source_col2, Bright_Source_col3, etc. For every strong and poorly deconvolved source, we need to provide a region file (.crtf). For each region (or direction), CASA will generate a mask and apply it to the images (.image, .model, .residual, etc.) which we can later use in `tclean` with `niter=0`, `calcpsf=False`, `calcres=False`. This run will predict the model for that particular source in the MS.

5. Once we generate all required MODEL columns then we can call QuartiCAL and perform DD calibration. QuartiCAL has many gain options for example, phase (P), amplitude (A), bandpass (B), complex gain (G), delay (K), etc. One can solve more than one gain together with QuartiCAL. For each of the gain types, we can select time and frequency cadence. In this work, we solve three (phase, delay, and complex) gain terms together; phase and delay terms solve for a direction-independent column, and complex gain for the direction-dependent column.

6. After performing the DD calibration, QuartiCAL will generate a residual column in MS. QuartiCAL will model and subtract the bright source(s) from the visibility data. This column can be imaged with `tclean` to get the final image. In the final image, the bright source is removed and hence one can see improvements in the artifacts. The dynamic range is much better than the self-calibration direction-independent map. In this work, we used CASA 6.6 and Quartical 0.2.0 versions. Currently, we are also testing the newer version of Quartical with added features (e.g. combining fields/scans in the calibration.)

3 VLASS observations

In this work, we used two VLASS data sets (VLASS3.1.sb43271439.eb43441449.59966.291735266204 and VLASS2.1.sb38489296.eb38554894.59062.39375707176). These data sets we downloaded from the archive.

(1) The VLASS3.1 data has bright 3C286 ($S_{3GHz} \sim 9.5$ Jy) at RA=13:31:08.28 and Dec=+30.30.32.96 and it causing strong artifacts in the observation. This strong artifact affects every field of the data. The VLASS QL image (covering the 3C286) was rejected in the QA. We processed the corresponding VLASS archival data of this QL image and ran the VLASS self-calibration pipeline on it. We used the same phase-center (J2000 13:32:18.5436 +30.29.59.904) as in the QL image, in the selfcal run. From this phase center, 3C286 is located 19' away. There are a total of 189 mosaic fields (same as in the QL image) in the final MS that are associated with only the VLASS image in the analysis.

(2) The another VLASS2.1 data has a bright ($S_{3GHz} \sim 1.7$ Jy) source at RA=2:31:45.89 and Dec=+13:22:54.71 causing the strong artifacts. In the NASA NED database, this source is identified as [HB89] 0229+131 (or 4C 13.14) QSO. The NED reported flux density is ~ 1.4 Jy at 2700 MHz. The QL image for this observation was also QA rejected due to the poor rms. The QL image, corresponding to this data, has the phase-center of J2000 RA=02:30:47.347, Dec=+13.30.0.000, and the bright source is 16' away from this center. There are a total of 229 fields in this VLASS image.

4 Result

In this section we show our 1st image (after bandpass and gain calibration), after self-calibration, and final peeling results for both above VLASS data. We downloaded the calibrated VLASS visibilities (by applying online automated CASA pipeline version 6.6.1-17—2024.1.1.22) of the two data sets. Then we ran the `tclean` on the CORRECTED_DATA column using the recommended cleaning parameters (from the VLASS pipeline) except uvrange and robust parameters. We used zero for both of these parameters. From this run, we generated the 1st image. Using this 1st map, we generated a mask with a sigma threshold of 8 and manually inspected the mask to include only real astronomical sources and not any artifacts. Using this mask, we ran again `tclean` and generated the 2nd image and first sky models. Then we ran self-calibration, without combining fields and spws. In mosaic observation, each field is independent, so we derived gain solutions per field and per spws to achieve higher SNR. Then we imaged the CORRECTED_DATA column which is self-calibrated and generated 3rd image. Since there is no faint or extended emission in both of these data, there is no need to update the mask. Using the final selfcal model, we ran QuartiCAL as mentioned in section 2. Finally, we imaged the residual data and generated the final DD calibration image. We show all of these results in Figures 1, 2, 3, and 4. Below we calculated image statistics.

(1) For our VLASS 3C286 data, we show 1st image (Fig. 1(a)), selfcal map (Fig. 1(b)) and after peeling image Fig. 2. We listed global, local (around bright 3C286 source) rms, and DR for these three images in Table 1. There is a factor of ~ 8 improvements around the bright 3C286 source after DD calibration (from 1st image). There is a factor of ~ 3 improvements after selfcal. Due to these improvements, there are 5 faint point sources visible around 3C286 (Fig. 2(b)) which were not visible in the other two maps.

(2) For other VLASS data in our analysis, we show 1st image (Fig. 3(a)), the selfcal map (Fig. 3(b)), and after peeling image in Fig. 4. We listed global, local (around bright source) rms, and DR for these three images in Table 1. In this data, there is a factor of 6 improvements around the bright source after DD calibration (from 1st image). There is a factor of ~ 2 improvements after selfcal. For these maps, we detected point and compact sources (with pybdsf software) and compared their fluxes and peak flux values. We show these plots in Figs 5 and 6, respectively.

Table 1: RMS and Dynamic Range (DR) comparisons for VLASS images before and after DD calibration.

VLASS dataset	Image type	Global RMS (μJy/beam)	Local RMS (mJy/beam)	DR (peak/rms)
3C286	1st Image	~100	~3.57	2380
	Self-Cal	~91	~1.19	7142
	After Peeling	~66	~0.44	19318
[HB89] 0229+131	1st Image	~151	~3.33	456
	Self-Cal	~144	~1.05	1447
	After Peeling	~143	~0.52	2923

5 Discussion

In VLASS observations, there are many bright (>100 mJy) sources limiting the dynamic range and preventing to detect or study of faint and low surface brightness objects, in the presence of strong artifacts. These artifacts around this bright source(s) cannot be removed by only cleaning or deconvolution processes. The probable reason is these sources are poorly calibrated due to their position in the beam, phase/amplitude errors, antenna pointing errors, baseline-based calibration errors, or their excessive brightness dominates the gain solutions in the self-calibration process. The artifacts from these poorly deconvolved sources are typically restricted within ~ 30' of the peak of the source, but sometimes they can extend artifacts up to 1 deg^2 in full VLASS image. For this type of situation, we developed a 'peeling' or DD calibration technique to model and subtract bright and problematic sources located toward particular direction. The QuartiCAL is a useful new calibration package that can be utilized with the CASA. We developed a Python script[3] that can be run inside the CASA environment to perform the peeling. Users only need to provide a region file that includes either one source or multiple sources. Then Python script will perform DD calibration for each of the sources and improve the image quality and dynamic range as shown above for VLASS data. However, even after the bright source peeling in the above examples, still, some moderate-level artifacts are still visible in the residual images. The reason could be the nature of mosaic observation and primary beam response to each of the fields. The location of the bright source is moving in each of the fields and hence characterizing it (with time and frequency) in every field is very difficult. Hence some of the fields may not accurately apply DD corrections to the source which leaves out residual artifacts and calibration errors in the final joint mosaic image. This issue is still under investigation and needs further testing. We also compared fluxes (and peak fluxes) of point sources, before and after peeling. We found scatter in fluxes for faint sources, but fluxes of bright sources are well compared before and after peeling. We found an average flux difference is ~ 12% for this VLASS mosaic data. In this analysis, we ran our peeling script on a NRAO luster. Typically Quartical takes 6 and half hours to complete DD calibration for ~ 200 VLASS fields with 16 spws. Including self-calibration and peeling, it takes ~ 40 hrs total time. This is a serial job and currently, Quartical is not usable with MPICASA.

6 Future plan

This Python script can be usable for any VLA data. So, there is a need to test it for other VLA data for different bands. In future, we will incorporate `gridder=awp2` in `tclean`. This gridder uses the aperture illumination models with azimuthally asymmetric beams, including squint correction, beam rotation, and W-projection. This will improve the input sky models and better constrain the calibration process. We are testing the latest version of Quartical (V 0.2.5) which has improvements in combining mosaic fields/scans in calibration to enhance the SNR. We will provide users with the latest CASA (v 6.7) with QuartiCAL installed in it.

[3] `https://github.com/viralp/casa_peel`

Acknowledgement

VP acknowledges Amy Kimball, John Tobin, and Steve Myers for their fruitful comments on the memo. VP also acknowledges Jonathan Kenyon and Oleg Smirnov for fruitful discussion.

References

Kenyon, J. S., Perkins, S. J., Bester, H. L., Smirnov, O. M., Russeeawon, C., & Hugo, B. V. 2025, Astronomy and Computing, 45, 100123

Kenyon, J. S., Smirnov, O. M., Grobler, T. L., & Perkins, S. J. 2018, MNRAS, 478, 2399, 1805.03410

Lacy, M. et al. 2020, PASP, 132, 035001, 1907.01981

Smirnov, O. M. 2011a, A&A, 527, A106, 1101.1764

——. 2011b, A&A, 527, A107, 1101.1765

Williams, P. K. G., Allers, K. N., Biller, B. A., & Vos, J. 2019, Research Notes of the American Astronomical Society, 3, 110

(a) VLASS 1st image around 3C286 region (VLASS 3.1).

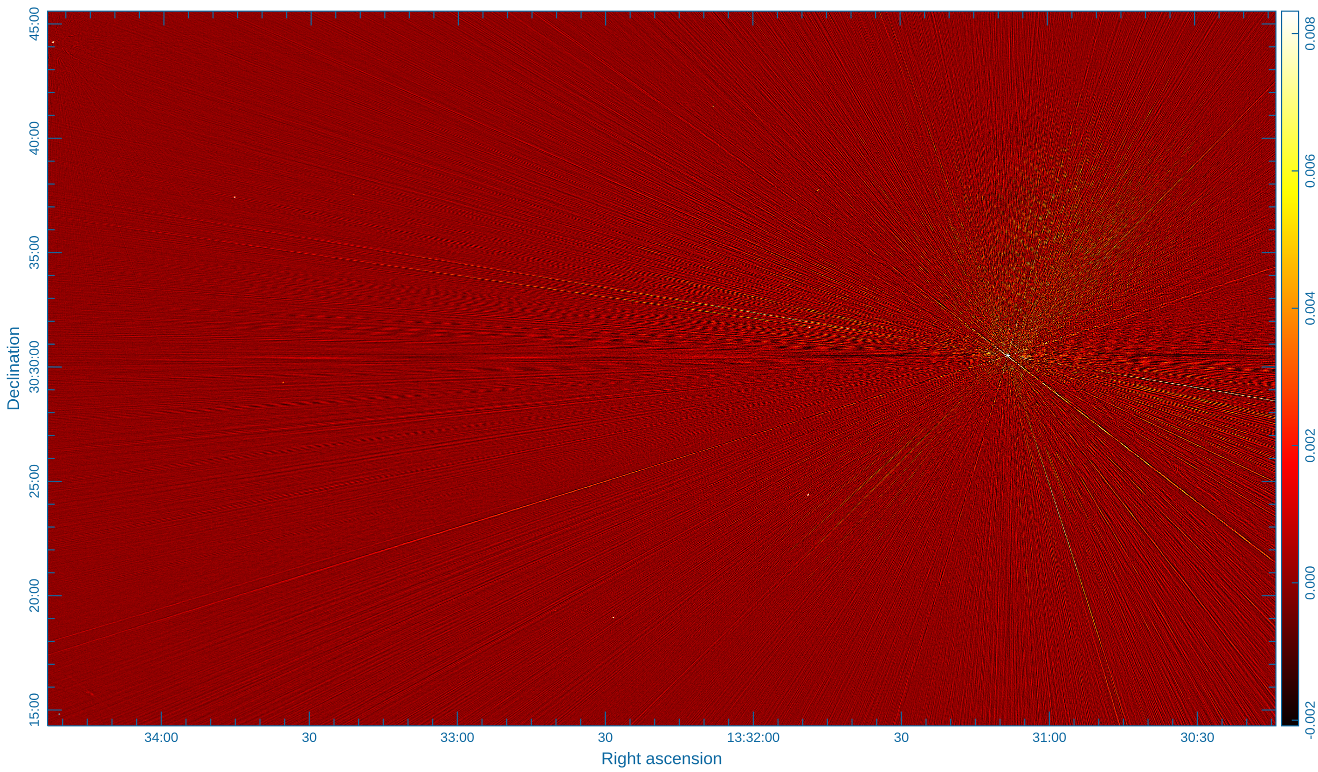

(b) Self-calibrated image of 1st map.

Figure 1: (a) and (b) are direction-independent calibrated images.

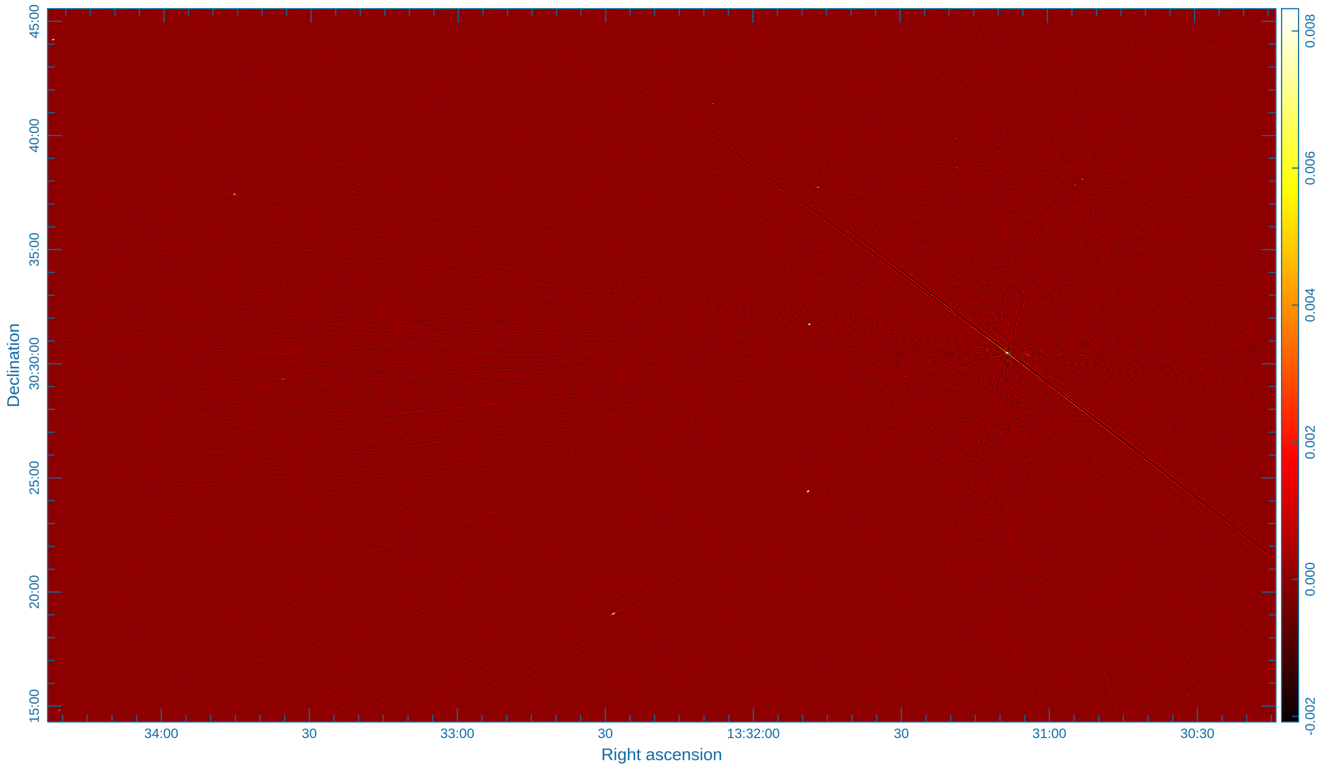

(a) Direction-dependent calibrated image. 3C286 is modeled and subtracted (peeled) from the data.

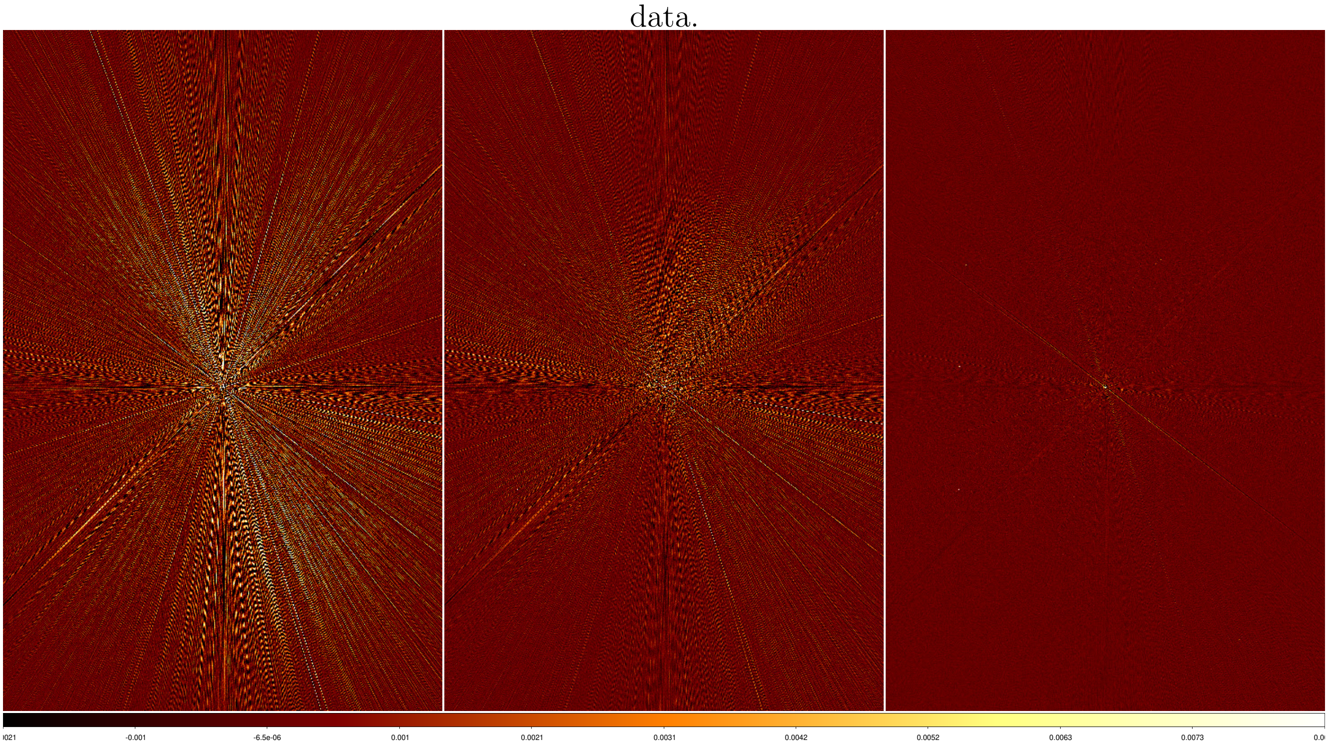

(b) Zoomed around 3C286 in left (1st map), middle (self-calibration map) and right (DD corrected map). The left image has DR = 2380, in middle DR = 7142, and in right DR = 19318.

Figure 2: (a) and (b) shows the direction-dependent calibrated image.

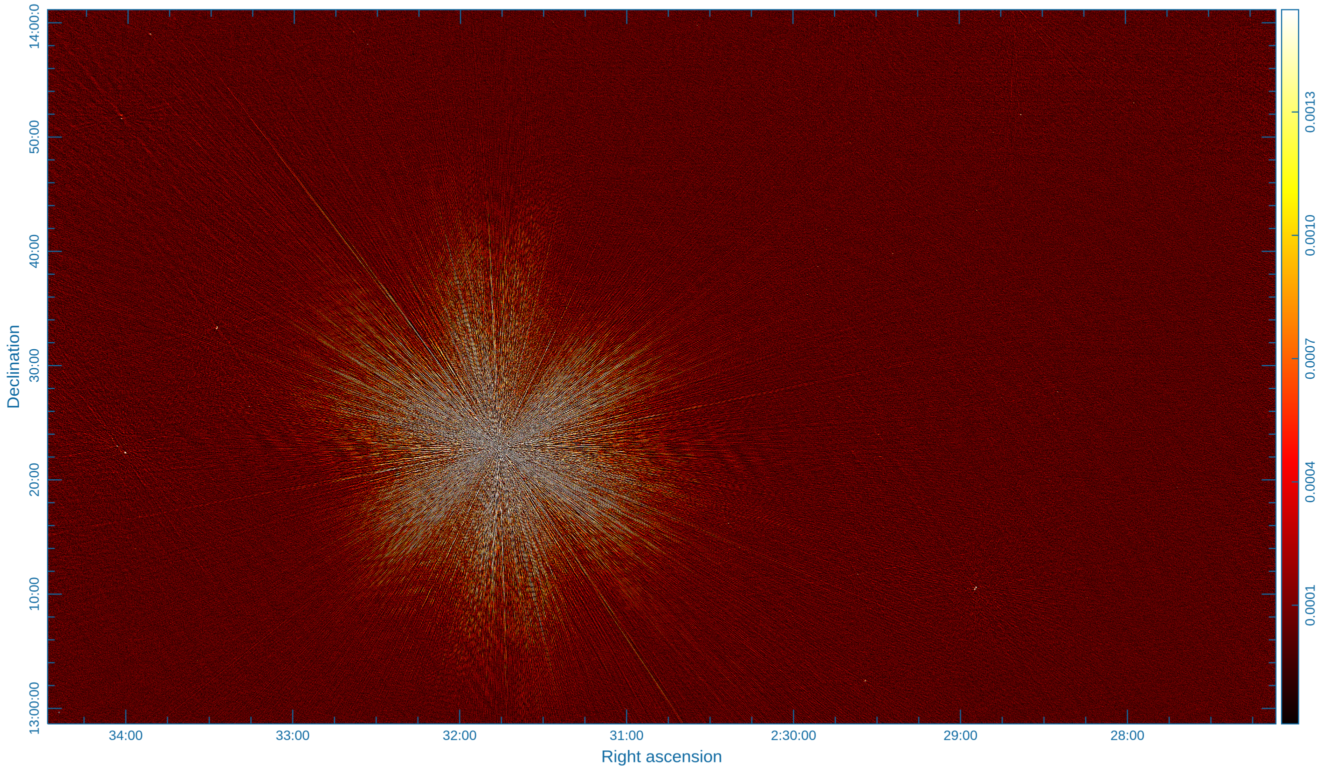

(a) 1st image around [HB89] 0229+131 (VLASS 2.1).

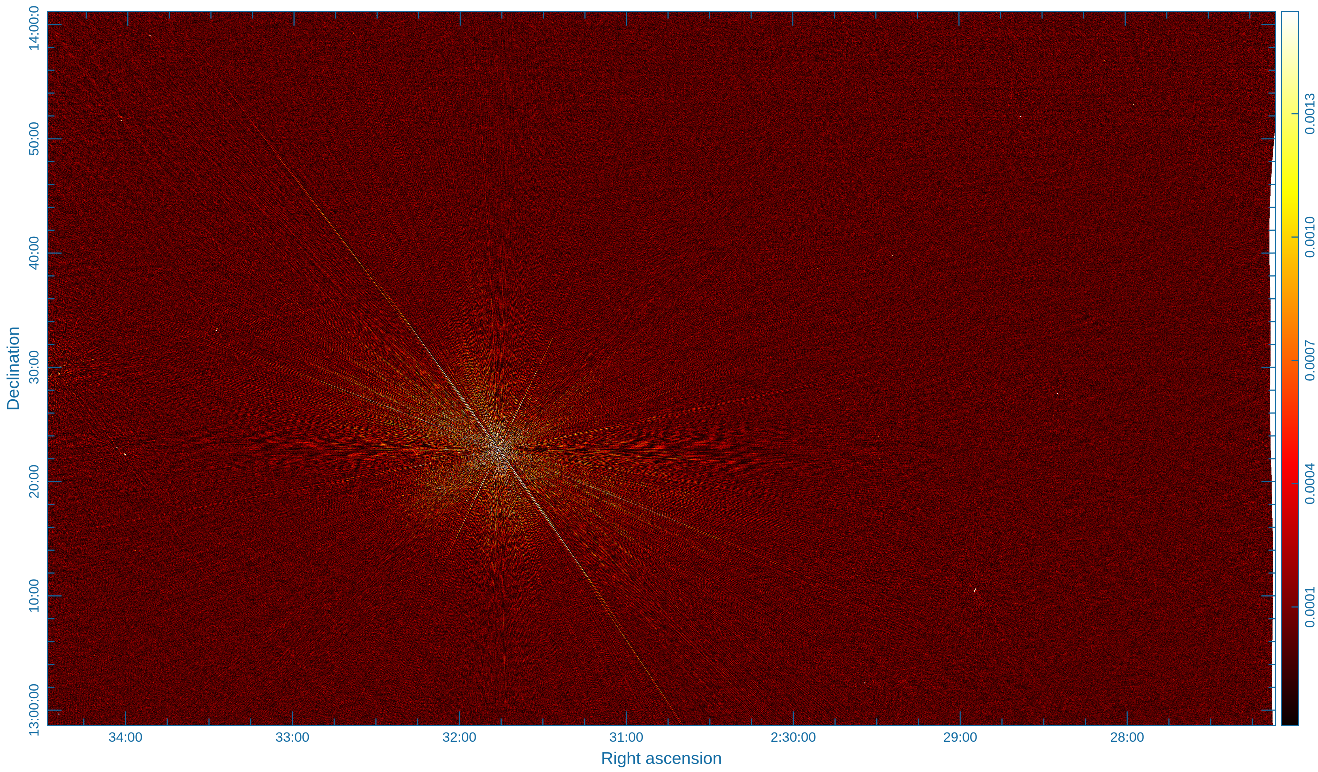

(b) Self-calibrated image.

Figure 3: (a) and (b) are direction-independent images.

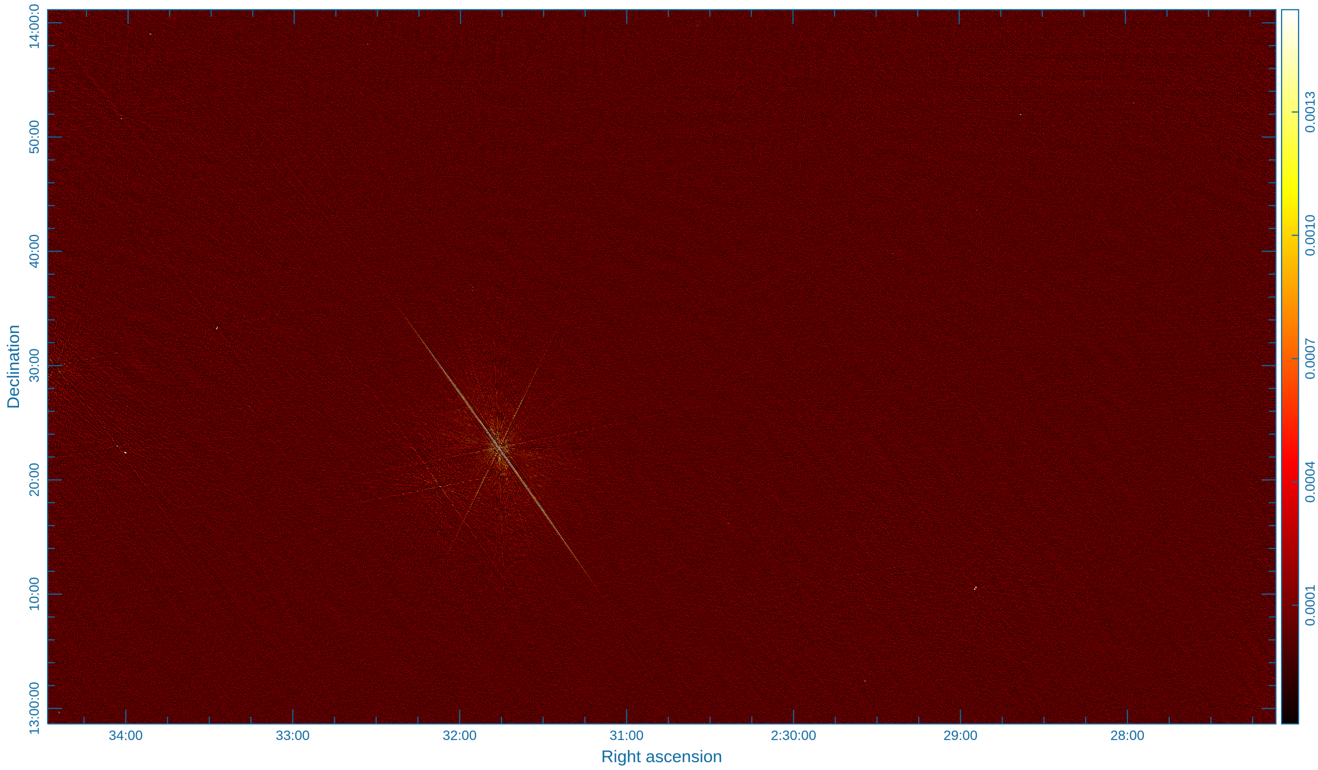

(a) Direction-dependent calibrated image.

Figure 4: (a) shows the direction-dependent calibrated image.

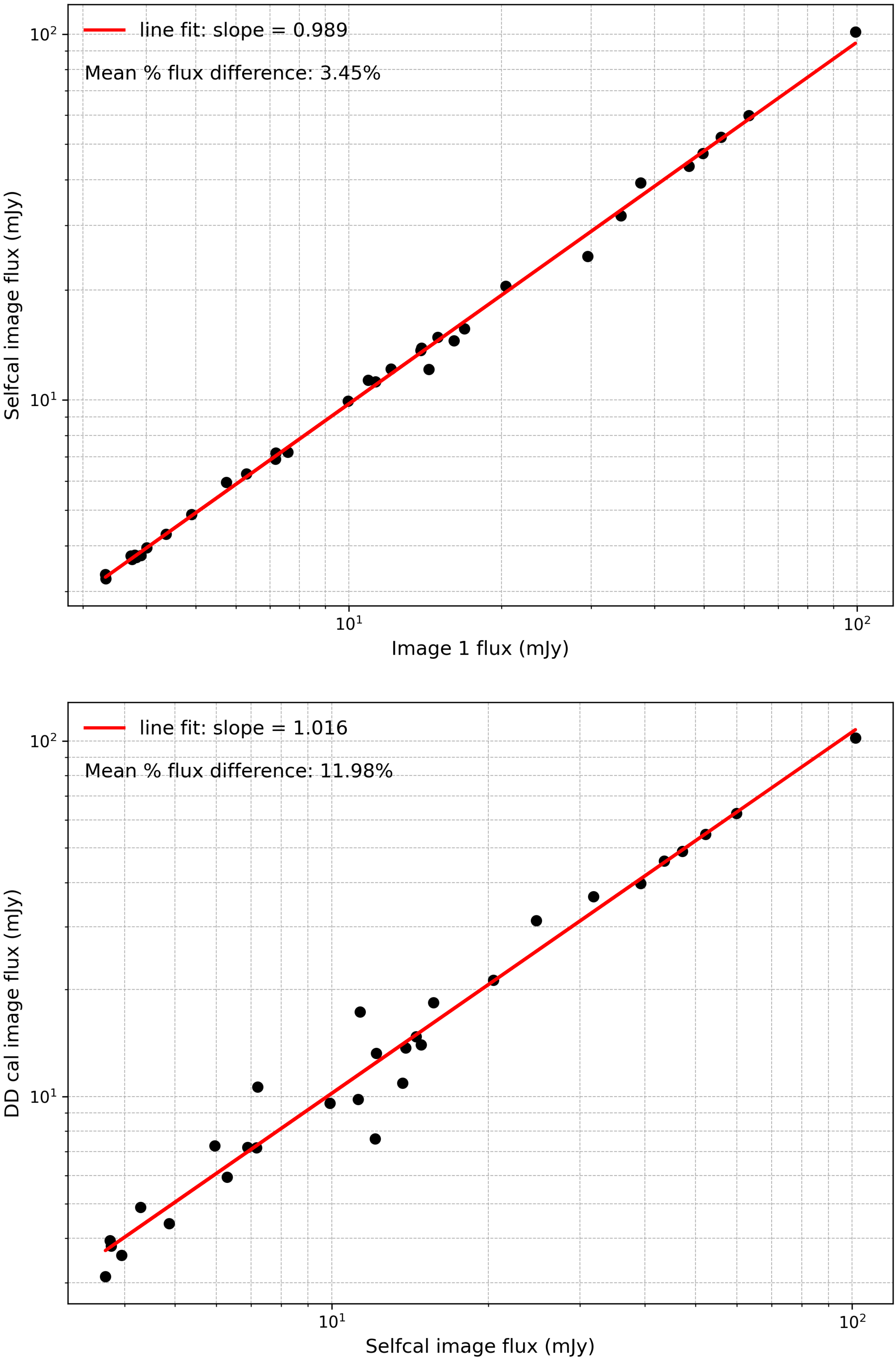

(Top) Flux comparison between image 1 and selfcal map. (Bottom) Flux comparison between selfcal map and DD cal map.

Figure 5: Flux values comparison between images.

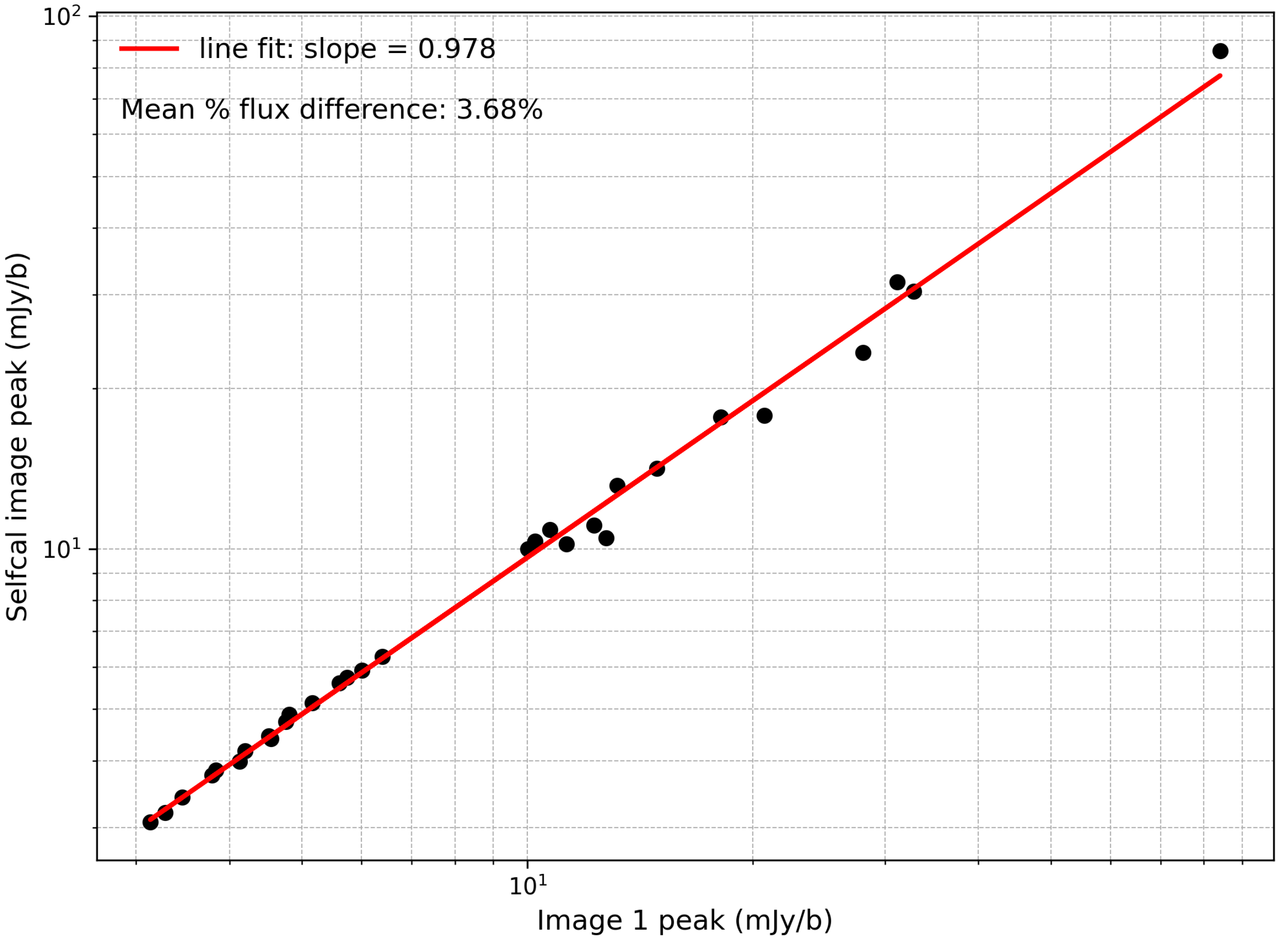

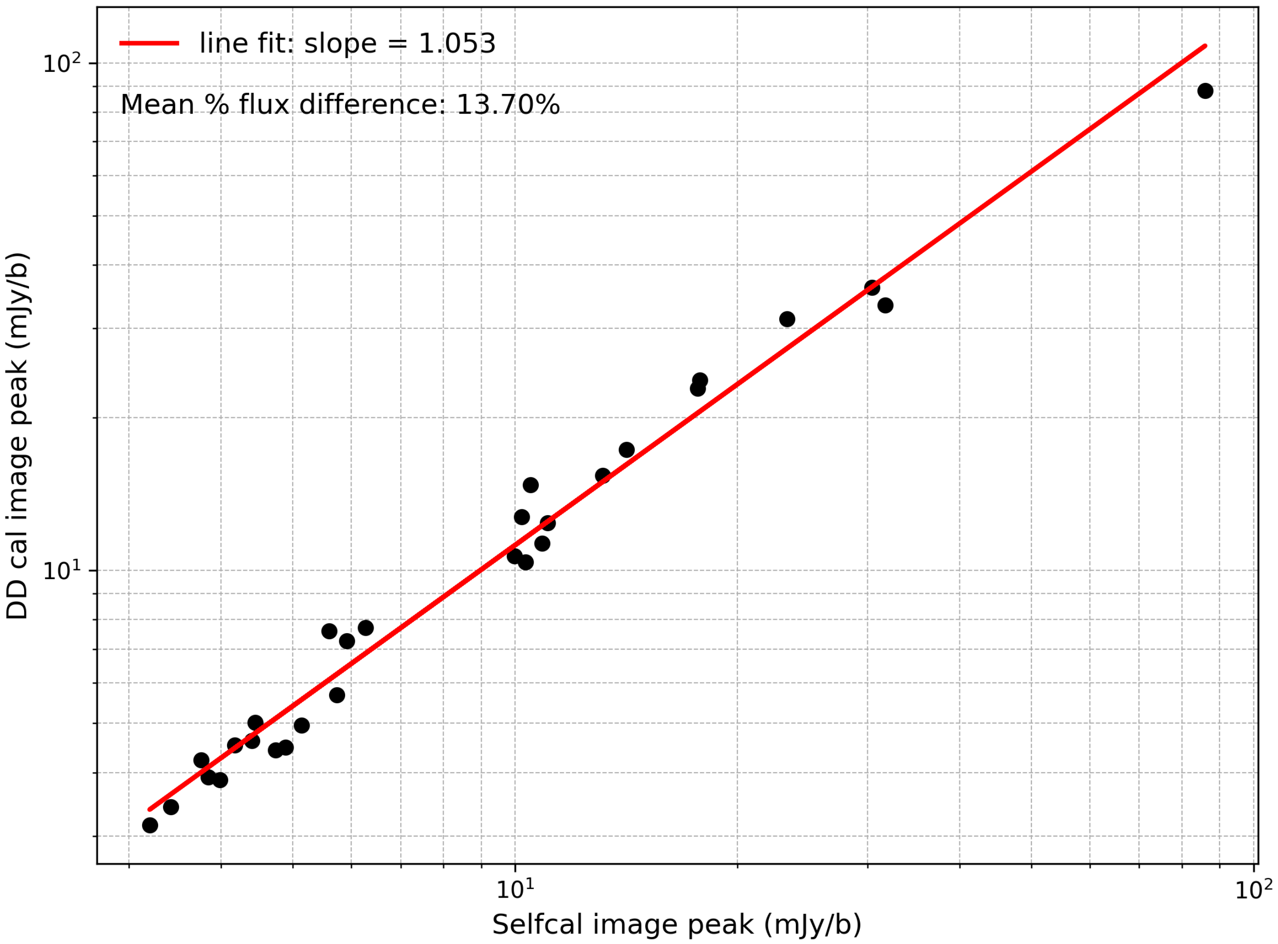

(Top) Peak flux comparison between image 1 and selfcal map. (Bottom) Peak flux comparison between selfcal map and DD cal map.

Figure 6: Peak flux values comparison between images.